On The Application Of Gibbs Equations In Determining The Relationships Of Vapour Pressures To Phase Diagrams Of The Reactive Chloride Systems

A.A. KIPOUROS, G. JARJOURA, G.J. KIPOUROS

Dalhousie University, Department of Mechanical Engineering,
Faculty of Engineering, 5269 Morris Street, PO Box 15000,
Halifax Nova Scotia B3H 4R2, CANADA

Corresponding author: georges@kipouros.ca

Abstract: Most of the phase diagrams reported in the literature have been determined in open atmospheric conditions indicating that the substances involved are not influenced by the presence of air and moisture. In these cases, the Gibbs phase rule is applied in its open condition of 1 atm pressure, and no special conditions need to impose. However, for many elements, such as all reactive metals, the phase diagrams are determined by conditions imposed to remove all the reactive actions of the presence of an atmosphere. In these cases, a special cell is needed to be constructed in a way that the material of construction of the cell and the absence of air is secured. The Gibbs phase rule is applied in its full mathematical formulation in those cases. The present publication reports on the determination of correct conditions to obtain meaningful results on the phase diagrams.

Key-words: Gibbs , thermodynamics, phase diagrams

Received: June 16, 2022. Revised: July 17, 2023. Accepted: August 27, 2023. Published: September 18, 2023.

1 Introduction

Alkali halides are known to absorb moisture, and in such cases, they may affect measurements of phase diagrams. The effects of reactions with containers may interfere with measurements. In case alkali halides are mixed with reactive metal halides, the mixtures and any amount of contained moisture not only will interfere with the measurements but also may lead to explosive situations as the measurements are performed in high temperatures as such cases are involved in the determination of phase diagrams of alkali halides and reactive metal halides. As these phase diagrams are critical in handling these materials, it is necessary to purify the alkali halides separately and the reactive halide, preferably in a glove box and then mixed and sealed under vacuum before measurements can be performed.
Prior to measurements, the substances used were purified. Alkali halides were dehydrated by heating under a vacuum for enough time to remove absorbed gases and moisture. Reactive metal halides, which are volatile, were loaded into a Pyrex tube, shown in Figure 1, and purified by passing through molten tin held in place by glass wool and condensing in the cold part of the apparatus. At the end of the purification, the apparatus was removed inside a dry box, and the metal halide was stored in clean containers for future use (1-11).

The true phase diagram, the phase diagram under its own equilibrium vapour pressure, was determined by the cooling curve technique. Because of this, the Gibbs Phase Rule, when it is applied, should be in its full form:

$$F = C - P + 2 \qquad [1]$$

Where

F=degrees of freedom
C = number of components
P= number of phases

Examining the phase diagram, each area is characterized by a number 1 to 6 and the liquid phase is characterized by the letter L.

Areas: 1, 2, 3, 4, 5, 6: F = 2 -3 +2 =1 degree of freedom
L: F= 2 – 2 +2 =2 degrees of freedom

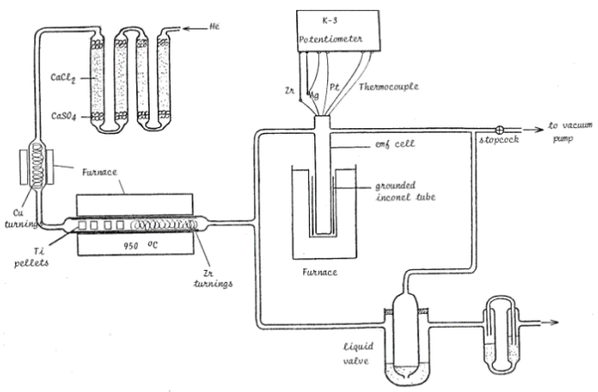

Figure 1. Schematic of the cell assembly

A special fixture for the determination of phase diagrams of the systems ACl-MCl4, where ACl is an alkali chloride and MCl_4 is a reactive metal chloride, is shown in Figure 2. Figures 3 and 4 show schematics of apparatuses related to the measurement of vapour pressure and a trail of purification of argon gas for continuous operations of the experiments.

Because the reactive metal halides have appreciable vapour pressure, the cooling curve measurements were carried out in sealed heart-shaped bulbs made of silica glass, as shown in Figure 2.

The typical phase diagram of the system ACl-MCl_4 is shown in Figure 5. The unusual characteristic of these diagrams relies on the fact that the vapour pressure of one end, alkali chloride, its melting point has only a few mmHg pressure while on the other end, the reactive chloride of such as zirconium and hafnium sublimes and does not melt but only when a very high pressure

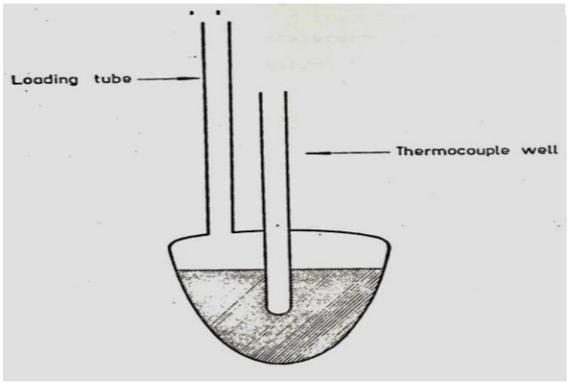

Figure 2. Fixture for the determination of phase diagrams of the systems ACl-MCl_4

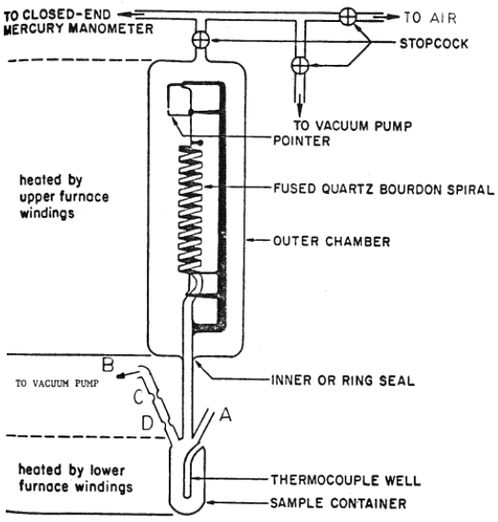

Figure 3. Schematic of the fixture for the determination of the phase diagrams of the systems

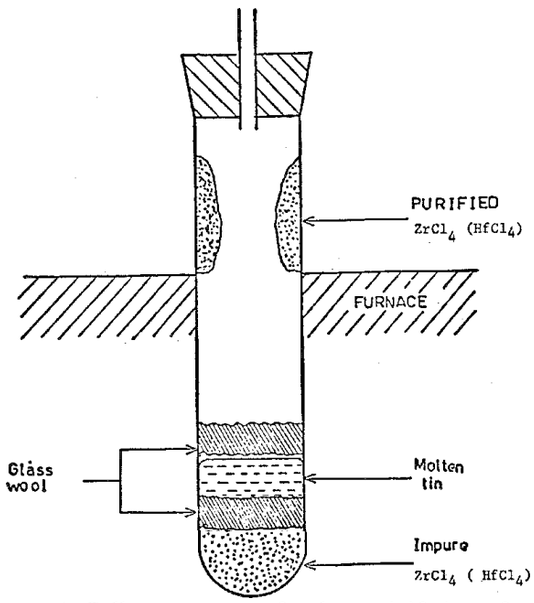

Figure 4. Cell arrangement for the puricifation of $ZrCl_4$ AND $HfCl_4$

2 Correlation of the vapour pressure to the phase diagram

The correspondence of these two diagrams is obtained from the following considerations. In the composition interval corresponding to the ACl-A_2MCl_6 subsystem, the thermal decomposition of A_2MCl_6 can be written in the following manner:

$$A_2MCl_{6(s\,or\,\ell)} = 2ACl_{(s\,or\,l)} + MCl_{4(v)} \qquad [2]$$

The free energy change for this reaction is given by

$$\Delta G = \Delta G° + RTln\left(\frac{a^2_{ACl}\cdot f_{MCl_4}}{a_{A_2MCl_6}}\right) \qquad [3]$$

Where fa_{ACl} and $a_{A_2MCl_6}$ represent the activities of ACl and A_2MCl_6 respectively, while f_{MCl_4} is the fugacity of MCl_4 vapour. In this treatment, it is assumed that the fugacity of MCl_4 may be considered equal to the partial pressure, an assumption justified by the temperatures and low pressures involved. The standard state for MCl_4 is its vapour at a pressure of 1 atm. For a condensed phase, the standard states of unit activity will be chosen as the pure solids at any temperature. The behaviour of solutions of different compositions can be followed as they are heated through the various labelled zones (12-16).

Zone 1, defined by $T < T_{eut}$ and $0 < X_{MCl_4} < XA_2MCl_6$, is characterized by the presence of two solids, AC1 and A_2MCl_6, and MCl_4 vapour. The decomposition reaction [1] may be written as

$$A_2MCl_{6(s)} = 2ACl_{(s)} + MCl_{4(v)} \qquad [4]$$

The free energy change for the decomposition reaction [4] takes the form

$$\Delta G = \Delta G_1^0 + RT\,ln\,P_{MCl_4} \qquad [5]$$

since both condensed phases are mutually insoluble and, therefore, at unit activity. At equilibrium $\Delta G = 0$, and equation [5] may be expressed as

$$RTlnP_{(MCl_4)} = -\Delta G_1^0 \qquad [6]$$

The Gibbs-Helmholtz equation gives for the temperature dependence of pressure in zone 1, the expression

$$\frac{\partial\, ln\, P_{MCl_4}}{\partial\left(\frac{1}{T}\right)_{p,n}} = -\frac{\partial\left(\frac{\Delta G_1^0}{RT}\right)}{\partial\left(\frac{1}{T}\right)} = -\frac{\Delta H_1^0}{R} \qquad [7]$$

Where ΔH_1^0 represents the enthalpy of decomposition of A_2MCl_6 into ACl and MCl_4, according to [4], when reactants and products are in their standard states. According to equation [4], assuming $\Delta C_P = 0$ a plot of $Ln\left(P_{MCl_4}\right)$ versus $\frac{1}{T}$ should be linear with slope $-\Delta H_1^0/R$. This implies that a single curve should represent the vapour pressures versus temperature relationship in zone 1 for all compositions.

In the zone labelled L, the all-liquid region, the decomposition reaction takes the form

$$\underline{A_2MCl_6}_{(\ell)} = 2\underline{ACl}_{(\ell)} + MCl_{4(v)} \qquad [8]$$

Where the line under A_2MCl_6 and ACl denotes that each of these compounds is in solution.

The equation for the free energy change for this reaction is

$$\Delta G = \Delta G_1^0 + 2RT\,ln\,a_{ACl} + RT\,ln\,P_{MCl_4} - RT\,ln\,a_{A_2MCl_6} \qquad [9]$$

At equilibrium $\Delta G=0$, and by rearranging the equation [11] the vapour pressure is given by

$$RT\,ln\,P_{MCl_4} = \Delta G_1^0 + RT\,ln\,a_{A_2MCl_6} - 2RT\,ln\,a_{ACL} \qquad [10]$$

The temperature dependence of pressure is then

$$\frac{\partial\, ln\, P_{MCl_4}}{\partial\left(\frac{1}{T}\right)} = \frac{-\Delta H_1^0 + \overline{\Delta H}_{A_2MCl_6} - 2\overline{\Delta H}_{ACl}}{R} \qquad [11]$$

$\overline{\Delta H}_{A_2MCl_6}$ and $\overline{\Delta H}_{ACl}$ in equation [11] are the partial molar enthalpies of mixing of A_2MCl_6 and ACl with respect to the pure solids as reference states, while ΔH_1^0 is the standard enthalpy of decomposition of solid A_2MCl_6 into MCl_4 vapour and solid ACl, according to reaction [4], where the reactant and products are in their standard states. According to equation [11] and under the assumption that $\Delta Cp = 0$ a plot of Lnp_{MCl_4} versus $\frac{1}{T}$ should be linear with slope $-\Delta H_1^0 + \Delta H_{A_2MCl_6} - 2\Delta H_{ACl)}/R.\Delta H_1^0$ for the decomposition reaction [9] is expected to be large relative to the partial molar enthalpies $\overline{\Delta H}_{A_2MCl_6}$ and $\overline{\Delta H}_{ACl}$.

Therefore, the slope of Lnp_{MCl_4} versus $\frac{1}{T}$ should be negative.

The standard state reaction may be written as

$$A_2MCl_{6(s)} = 2ACl_{(s)} + mcl_{4_{(v,l\ \ at)}} \qquad [12]$$

A plot of the temperature dependence of the partial pressure of MCl_4 over a solution, which upon heating passes successively through zones 1 and L, consists of two lines having different slopes. Such a solution that corresponds to exactly the eutectic composition indicated as X_2 in Figures [2] and [3]

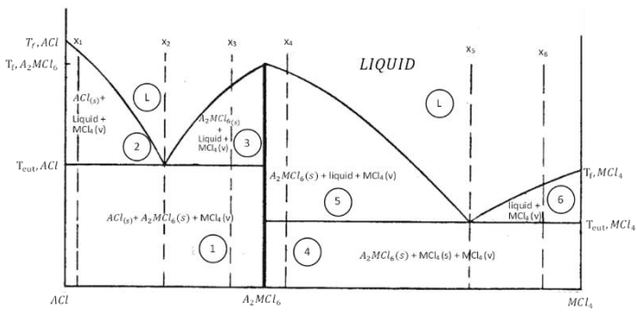

Figure 5. Schematic representation of the phase diagram of ACl-MCl_4

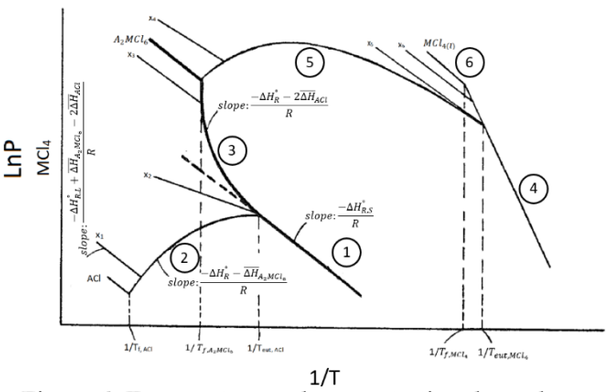

Figure 6. Temperature and concentration dependence of vapour pressure in the ACl-MCl_4 system

Region 2 represents the alkali-rich part of the ACl-A_2MCl_6 subsystem with boundaries the liquidus and eutectic temperatures. There are three phases present, namely MCl_4 vapour, molten solution. ACl-A_2MCl_6 and pure solid ACl. The general decomposition reaction, represented by equation [2] can be written for this zone as

$$\underline{A_2MCl_6}_{(\ell)} = 2ACl_{(\ell,saturated\ with\ \ ACl_{s)}} + MCl_{4_{(v)}} \qquad [13]$$

The free energy change for the above reaction can be expressed as

$$\Delta G_2 = \Delta G_1^0 + RT\ ln\ P_{MCl_4} - RT\ ln\ \alpha_{A_2MCl_6} \quad [14]$$

Where, ΔG_1^0 refers to the same standard reaction as previously. The absence of an activity term for ACl in this equation is due to the fact that although ACl is present as a liquid, it is in equilibrium with solid ACl and therefore its activity is unity. The temperature dependence of the partial pressure of MCl_4 is

$$\frac{\partial\ ln\ P_{MCl_4}}{\partial\left(\frac{1}{T}\right)} = \frac{-\Delta H_1^0 + \overline{\Delta H}_{A_2MCl_6}}{R} \qquad [15]$$

Where ΔH_1^0 is the enthalpy of decomposition of solid A_2MCl_6 into solid ACl and MCl_4 vapour when the reactants and products are in their standard states and $\overline{\Delta H}_{A_2MCl_6}$ represents the partial molar enthalpy of mixing of pure solid A_2MCl_6 in molten A_2MCl_6 - ACl

Figure [6] shows a plot of the temperature dependence of the partial pressure of MCl_4 over a solution of composition X_1,where X_1 is shown in the phase diagram of Figure 6. The plot consists of two straight lines joined by a curve which intersects them at $\frac{1}{T_{Liquidus}}$ and $\frac{1}{T_{eut.ACl}}$ the curved part of this plot illustrates what happens when the solution of the initial composition X_1 is heated through zone 2. Upon entering zone 2, solid AC1 is in equilibrium with a molten solution of ACl - A_2MCl_6 having the eutectic composition X_2. As the temperature increases the composition of the liquid solution ACl - A_2MCl_6 changes following the liquidus line of phase diagram. In effect the liquid solution, always in equilibrium with solid ACl, is continuously depleted in A_2MCl_6 and therefore for the temperature range between, the boundary values of $\frac{1}{T_{eut.ACl}}$ and $\frac{1}{T_{Liquidus}}$ its vapour pressure is being lowered. The degree of curvature will depend upon the composition-dependence of the partial molar enthalpy of mixing, $\overline{\Delta H}_{A_2MCl_6}$ which appears in equation [15].

The complex-compound-rich part of the ACl - A_2MCl_6 subsystem, labelled 3 in Figure 5, is defined by the liquidus and eutectic temperatures. The phases present are MCl_4. vapour, a molten, solution of ACl - A_2MCl_6 and pure solid A_2MCl_6. The decomposition reaction is

$$A_2MCl_{6\left(\ell,saturated with A_2MCl_{6(s)}\right)} = 2ACl_{(\ell)} + MCl_{4_{(v)}} \qquad [16]$$

Where the line under AC1 denotes that it is in solution.

The free energy change for the above reaction is

$$\Delta G_3 = \Delta G_1^0 + 2RT\ ln\ a_{ACl} + RT\ ln\ P_{MCl_4} \qquad [17]$$

The activity of A_2MCl_6 in the saturated solution is unity. The Gibbs-Helmholtz equation is

$$\frac{\partial\ ln\ P_{MCl_4}}{\partial\left(\frac{1}{T}\right)} = \frac{-\Delta H_1^0 - \overline{2\Delta H}_{ACl}}{R} \qquad [18]$$

where ΔH_1^0 refers to the standard enthalpy of decomposition of solid A_2MCl_6 into solid ACl and vapour MCl_4, and is the partial molar enthalpy of mixing of pure solid ACl in molten A_2MCl_6 - ACl.

Considerations, similar to those applied for zone 2, could be used in zone 3 to predict the temperature dependence of the partial pressure of MCl_4 for solutions heated through this zone. Figure 6 illustrates the behaviour of a solution of composition X_3. The plot again consists of two straight segments joined by a curved section, intersecting them at $\frac{1}{T_{Liquidus}}$and $\frac{1}{T_{eut.ACl}}$. As the initial solution of composition X_3 is heated to the eutectic temperature, pure solid A_2MCl_6 is in equilibrium with a liquid solution of ACl - A_2MCl_6 of the eutectic composition. As the temperature increases, the composition of the liquid which is in equilibrium with pure solid A_2MCl_6 is changing along the liquidus phase diagram. That is, it becomes enriched in A_2MCl_6.Therefore the vapour pressures, in the temperature range $\frac{1}{T_{eut.ACl}}$to $\frac{1}{T_{Liquidus}}$, of the initial composition X_3, increase to values higher than at the eutectic composition. The degree of curvature will depend upon the composition dependence of the partial molar enthalpy of mixing $\overline{\Delta H}_{ACl}$ which appears in equation [18].

The limits of the curves associated with zones 2 and 3 of the ACl - A_2MCl_6 subsystem are shown in Figure 6. Zone 2 ends at $\frac{1}{T_{fus,ACl}}$ with a pressure equal to that of pure ACl at the melting point, while the limit for zone 3 is the melting point of the complex compound A_2MCl_6.

The A_2MCl_6 - MCl_4 subsystem is characterized by pressures much higher than those encountered in the ACl - A_2MCl_6 subsystems , but the shape of the P-T curves can still be predicted, although using different considerations.

In region 4, defined by $T < T_{eut.,MCl_4}$and $X_{A_2MCl_6} < T_{MCl_4} < 1.0$ there are three phases present, MCl_4 vapour and the two solids, MCl_4 and A_2MCl_6, which are mutually insoluble.

From phase relation considerations the chemical potential of MCl_4 must be independent of composition in this zone. Since both A_2MCl_6 and MCl_4 are present in the solid form, the vapour pressure of pure solid MCl_4 is expected to be several orders of magnitude greater than the partial pressure of MCl_4 produced by the decomposition of A_2MCl_6. Thus, the decomposition reaction of A_2MCl_6 is suppressed by the dominant vapour pressure of the sublimation of pure MCl_4.

In region 5, pure solid A_2MCl_6 is in equilibrium with a liquid solution of A_2MCl_6 – MCl_4 and MCl_4 vapour. The decomposition reaction is that given by equation [18] and the treatment followed in zone 3 may be extended to cover this region. The liquid in equilibrium with pure A_2MCl_6 changes composition with temperature, being depleted of MCl_4 as T increases. The Plot of $Ln(P)$ versus $\frac{1}{T}$ plot should be a curve as shown in Figure [6] for a solution of initial composition X4.

Finally, in region 6 the phases present are MCl_4 vapour, a molten solution of A_2MCl_6 and MCl_4, and solid MCl_4. Since the liquid A_2MCl_6 – MCl_4 solution is saturated with solid MCl_4, the pressure over the system is that of pure solid MCl_4. This is illustrated, by the th plot of $Ln(P)$ versus $\frac{1}{T}$ for a solution of initial composition X_6. The limit of this region is the hypothetical melting of pure solid MCl_4 under its own pressure. This is shown in Figure 7 which also presents the composite of pressure curves for the entire ACl – MCl_4 system.

A typical phase diagram of the binary system ACl – MCl_4, where ACl represents an alkali chloride and MCl_4 zirconium or hafnium tetrachloride has been shown in Figure 6 and it indicates the formation of congruently melting compounds of the type A_2MCl_6. As discussed in a previous section the ACl-$ZrCl_4$ system may be divided into two subsystems: the zirconium tetrachloride-rich region A_2ZrCl_e-$ZrCl_4$ and the alkali chloride-rich region ACl-A_2ZrCl_6.

In the A_2ZrCl_e-$ZrCl_4$ subsystem, in the temperature range where the system is liquid, the vapour pressure is higher than one atmosphere due to the predominance of the molecular zirconium tetrachloride. Due to the high pressures involved, this part of the phase diagram is unsuitable for the electrolytic recovery of the metal.

Low vapour pressures of $ZrCl_4$ characterize the alkali chloride-rich side of the ACl-$ZrCl_4$ phase diagram. This is mainly due to the stabilizing effect, that the formation of the complex compound A_2ZrCl_6 has. The measured vapour pressures indicate that the subsystem ACl-A_2ZrCl_6 is attractive for electrolytic purposes. For low concentrations of A_2ZrCl_6 in ACl, which is the practice in electrolysis, the theory discussed in the previous section predicts that the vapour pressures of $ZrCl_4$ over the melt would be particularly low. Furthermore, it is expected that the larger the size of the alkali cation present, the greater the stability of the solution would be. Excluding economic considerations, the alkali chlorides to be used as primary components for stabilizing $ZrCl_4$ should be potassium or cesium chlorides.

The method for the preparation of the compounds was developed in the laboratory [(1)]. The reaction between an alkali chloride (ACl) and Zr or Hf tetrachlorides (MCl_4) is given as:

$$2ACl_{(S)} + MCL_{4(V,1\,atm)} = A_2MCL_{6(S)} \qquad [19]$$

in which a known amount of ACl ground to -325 mesh is reacted with an excess of purified MCI_4 vapour at 1 atm pressure. By weighing the salt after the reaction the stoichiometry of the product can be accurately determined. Identification is also achived by x-ray and nutron activation analysis [(3)]

The compounds were produced in a two-compartment cell as shown in Figure 7. The procedure was the following: Zirconium (or hafnium) tetrachloride was loaded into one compartment while finely divided anhydrous alkali chloride powder, exactly weighed,

was loaded into a Pyrex boat placed in the other. The large end of the reaction tube was sealed and the cell was evacuated. Then the cell was flamed sealed under vacuum and placed into the two compartment furnace assembly.

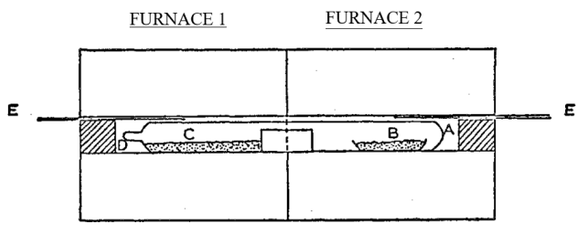

Figure 7. Reaction cell arrangement for the syntheses of the alkali hexachlorozirconates and Hexachlorohafnates

The ACl side of the cell was heated to 485°C while that of the tetrachloride was maintained at about 330°C when it was loaded with $ZrCl_4$, or, at 320°C when it was loaded with hafnium tetrachloride. At these temperatures the corresponding vapour pressures over the solid tetrachlorides are about 1 atm.

After a 4-day reaction period the side of the cell containing the compound was cooled to 350°C and after that both furnaces were cooled down stepwise by 30°- 40°C starting with the furnace containing the tetrachloride.

After cooling the reaction tube was opened in the dry box. The product of the reaction was weighed and if the reaction did not correspond to a $ACl/ZrCl_4$ (or $ACl/HfCl_4$) molar ratio of 2:1, the solid was ground in a dry box and rereacted.

This method of preparing the A_2MCl_6 compounds in a two-compartment furnace and cell assembly, overcomes the disadvantages of the any other method, because the possible products of hydrolysis of the chlorides remain behind on the tetrachloride side of the cell and not contaminate the final product. Furthermore the present method direct evidence for the extent of the reaction and the stoichiometry of the compounds is thus established.

Similar calculations were applied in the dehydration of $MgCl_2.6H_2O$ and $NdCl_3.6H_2O$ hydrates for the production of magnesium and neodymium metals (17-20).

3 Conclusions

Through a vigorous thermodynamic analysis using the Gibbs fundamental equations. Gibbs free energy, Gibbs phase rule and Gibbs-Helmholtz equation the vapour pressures can be calculated from the phase diagram information. This information is very important for the design of an electrolytic cell to produce the reactive metals from a melt containing alkali halide electrolyte to which the reactive metal halide is dissolved.

References

[1]. G.J. Kipouros, Separation of Hafnium from zirconiumby reaction of mixed tetrachloride vapours with solid potassium chloride, M.A.Sc., University of Toronto, (1976).

[2]. G.J. Kipouros, Electrorefining of zirconium metal in alkali chloride and alkali fluoride electrolytes and thermodynamic properties of some alkali-metal hexachlorozirconate and heachlorohafnate compounds, PhD Thesis, University of Toronto, (1982).

[3]. G.J. Kipouros and S.N. Flengas, "Equilibrium Decomposition Pressures of the Compounds K_2ZrCl_6 and K_2HfCl_6 ", Can. J. Chem., 56, 1549-1554 (1978).

[4]. G.J. Kipouros and S.N. Flengas, "Equilibrium Decomposition Pressures of the Compounds Na_2ZrCl_6 and Na_2HfCl_6 ", Can. J. Chem., 59, 990-995 (1981).

[5]. C.A. Pickles, G.J. Kipouros, R.G.V. Hancock and S.N. Flengas, "Quantitative Determination of Hafnium in Mixtures of Zirconium-Hafnium Hexachloro Alkali Compounds by Neutron Activation Analysis and X-ray Fluorescence", Can. J. Chem, 61, 2189-2191 (1983).

[6]. G.J. Kipouros and S.N. Flengas, "Equilibrium Decomposition Pressures of the Compounds Cs_2ZrCl_6 and Cs_2HfCl_6 and X-ray Identification of Na_2HfCl_6, K_2HfCl 6 and Cs $_2HfCl_6$", Can. J. Chem., 61, 2183-2189 (1983).

[7]. G.J. Kipouros and S.N. Flengas, "Electrorefining of Zirconium Metal in Alkali Chloride and Alkali Fluoride Fused Salts", 164th Meeting, Electrochemical Society, Washington D.C., Oct. 9-14 (1984).

[8]. G.J. Kipouros and S.N. Flengas, "Electrorefining of Zirconium Metal in Alkali Chloride and Alkali Fluoride Fused Electrolytes", J. Electrochem. Soc., 132, 1087-1098 (1985).

[9]. G.J. Kipouros and D.R. Sadoway, "The Chemistry and Electrochemistry of Magnesium Production" in Advances in Molten Salt Chemistry, Vol. 6, Edited by G. Mamantov, C.B. Mamantov and J. Braunstein, Elsevier, Amsterdam, pp. 127-209 (1987).

[10]. S.N. Flengas, G.J. Kipouros and P. Tumidajski, "Thermodynamic and Electrochemical Behaviour of Charge Fused Salt Solutions Suitable for the Electrolytic Recovery of Reactive Metals", International Symposium on Thermodynamics and Electrochemistry, November 20-22, Indira Ghandi Atomic Research Center, Kalpakkam, India (1989).

[11]. G.J. Kipouros and S.N. Flengas, "On the Mechanism of the Production of Zirconium and Hafnium Metals by Fused Salt Electrolysis", Proc. Seventh International Symposium on Molten Salts, Ed. S.N. Flengas, C.L. Hussey, Y. Ito and J.S. Wilkes. The Electrochemical Society, Pennington, NJ, Vol. 90-17, pp. 626-651 (1990).

[12]. G.J. Kipouros, "Bibliography of Electrochemistry", Internal Report, M.I.T., April 1983 (Revised, Dalhousie, January 2000).

[13]. G.J. Kipouros and S.N. Flengas, "Reversible Electrode Potentials for the Formation of Solid and Liquid Chlorozirconate and Chlorohafnate compounds", Can. J. Chem., 71, 1283-1289 (1993).

[14]. G.M. Photiadis, G.A. Voyiatzis and G.J. Kipouros, "Coordination of Lanthanide and Actinide ions in Fused Chloride solvents: Raman Spectra of Molten $NdCl_3$-ACl and $ThCl_4$ - ACl mixtures (A=Alkali)", 1994 EUCHEM Conference on Molten Salts , Bad Herrenald, Germany, August 21-26 (1994).

[15]. G.J. Kipouros and D.R. Sadoway, “Towards New Technologies for the Production of Lithium”, JOM, 50, (5), 24-26, (1998).

[16]. G.J. Kipouros and D.R. Sadoway, "A thermochemical analysis of the production of $MgCl_2$”, Journal of Light Metals, 1 (2), 111-117 (2001).

[17]. G. Jarjoura and G.J. Kipouros, “Investigation of the Effect of Nickel on Copper Anode PassiVation in a Copper Sulfate Solution by EIS”, J. Appl.. Electrochem., 36, 691-70 (2006).

[18]. W.D. Judge and G.J. Kipouros, “Prediction of hydrogen chloride pressure to avoid hydrolysis in the dehydration of dysprosium trichloride hexahydrate ($DyCl_3.6H_2O$)”,*Can. Metall. Quart*., 52,(3), 303-310 (2013).

[19]. G.J. Kipouros, “Dehydration of Magnesium Chloride Hexahydrate”, Ralph Lloyd Harris Memorial Symposium, Ed. Cameron L. Harris, Sina Kashani-Nejad and Matthew Kreuh, Materials Science and Technology (MS&T) 2013, 11-23 (Invited, keynote), (2013).

[20]. R.J. Roy and G.J. Kipouros, "Estimation of Vapour Pressures of Neodymium Trichloride Hydrates", Thermochimica Acta, 178, 169-183 (1991).